

Antifreezes Act as Catalysts for Methane Hydrate Formation from Ice**

Graham McLaurin, Kyuchul Shin, Saman Alavi, and John A. Ripmeester*

Abstract: Contrary to the thermodynamic inhibiting effect of methanol on methane hydrate formation from aqueous phases, hydrate forms quickly at high yield by exposing frozen water–methanol mixtures with methanol concentrations ranging from 0.6–10 wt% to methane gas at pressures from 125 bars at 253 K. Formation rates are some two orders of magnitude greater than those obtained for samples without methanol and conversion of ice is essentially complete. Ammonia has a similar catalytic effect when used in concentrations of 0.3–2.7 wt%. The structure I methane hydrate formed in this manner was characterized by powder X-ray diffraction and Raman spectroscopy. Steps in the possible mechanism of action of methanol were studied with molecular dynamics simulations of the 1h (0001) basal plane exposed to methanol and methane gas. Simulations show that methanol from a surface aqueous layer slowly migrates into the ice lattice. Methane gas is preferentially adsorbed into the aqueous methanol surface layer. Possible consequences of the catalytic methane hydrate formation on hydrate plug formation in gas pipelines, on large scale energy-efficient gas hydrate formation, and in planetary science are discussed.

Clathrate hydrates are crystalline inclusion compounds where guest molecules of suitable size are incorporated in cages formed by hydrogen-bonded water molecules. Three major families of hydrate structures are known, with the actual structure determined mainly by the size of the guest molecules.^[1] All three structures, mainly with hydrocarbon guests, are found naturally, although the cubic structure I (sI) methane hydrate is by far the predominant naturally occurring hydrate found both offshore on continental margins and under the permafrost.^[2] Hydrates are also a costly and potentially dangerous problem for the oil and gas industry because of plug formation in pipelines.^[3] Much effort has gone into the prevention of their formation as part of the practice of flow assurance, with the use of thermodynamic inhibitors such as methanol and ethylene glycol, as well as low dosage

kinetic inhibitors.^[3] The industrial scale synthesis of methane hydrate for large-scale transportation of methane is a topic attracting recent interest. Yet another, but more speculative area of interest is the possibility of methane clathrate hydrates in extraterrestrial space, especially on icy moons such as Titan where the presence of methane and water, as well as methanol and ammonia make for interesting possibilities of a variety of stoichiometric and clathrate hydrates.^[4,5]


Classically, hydrate guests were thought to interact with the hydrate cages mainly in a hydrophobic manner.^[6] However, the discovery of many water-soluble guests suggests that a measure of hydrophilic behavior does not disqualify a properly sized molecule from becoming a hydrate guest. Since hydrate lattice stability depends on the totality of the guest–host interactions, the guests collectively need to achieve a balance of the hydrophilic and hydrophobic guest–host interactions suitable for stable hydrate formation, and this can be achieved in various ways. For instance, some alcohols and amines not known to form clathrate hydrates can be encouraged to do so by using a “helpgas”, usually a small hydrophobic molecule to give a stable hydrate phase.^[7] By the same token, small molecules that interact strongly with water such as methanol and ammonia, which do not form hydrates at near-ambient temperatures, can be incorporated into hydrates along with a more hydrophobic guest that forms a stable hydrate.^[4,5] It is interesting to note that methanol has been used as hydrate inhibitor for some 70 years^[8] with the models used to predict hydrate formation in the presence of methanol assuming that methanol does not take part in hydrate formation in use since 1981.^[9]

Recent work has shown that a pure ammonia clathrate hydrate can be prepared at low temperatures, however this has not been possible for methanol.^[4,5] When preparing methanol- or ammonia-containing hydrates by annealing vapor deposits at low temperature, clathrate formation took place at much lower temperatures than when the vapor deposition involved only water and hydrophobic molecules (CH₄, Xe, O₂, N₂). We now extend our work on the activity of ammonia and methanol in hydrate formation from ice to relatively high temperatures. The formation of hydrate for energy gas storage (CH₄, H₂), greenhouse gas storage (CO₂), and gas separation (CO₂ from flue gas and synthesis gas) applications have been well-documented and hydrate formation for such applications is usually a rather inefficient and costly process involving stirred high-pressure reactors, low yields and solid–liquid separation.^[10] To improve the efficiency of hydrate formation, a variety of fixed bed reactors are being explored.^[10] The methodology presented in this work has potential to provide a simpler, faster, and more energy efficient route to the synthesis of these clathrate

[*] G. McLaurin, Dr. S. Alavi, Dr. J. A. Ripmeester
National Research Council of Canada
100 Sussex Drive, Ottawa (Canada)
E-mail: john.ripmeester@nrc-cnrc.gc.ca

Dr. K. Shin
Division of Ocean Systems Engineering
Korea Advanced Institute of Science and Technology
Daejeon, 305-701 (Republic of Korea)

[**] The authors acknowledge the support of the National Research Council of Canada.

 Supporting information for this article, including experimental and simulation protocols, is available on the WWW under <http://dx.doi.org/10.1002/anie.201403638>.

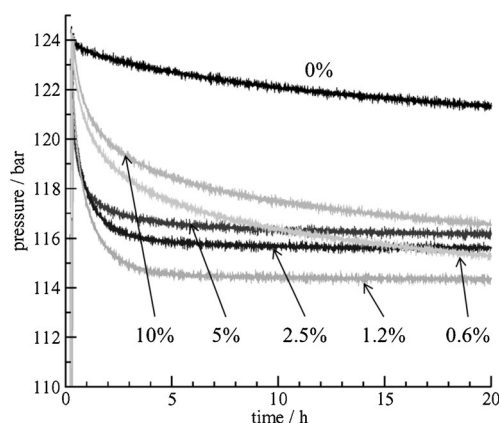


Figure 1. Pressure drop versus time for powdered frozen solutions containing different amounts of methanol in the initial water solution at 253 K.

hydrates. Here we propose an efficient solid–gas reaction for hydrate formation as catalyzed by methanol or ammonia, and propose steps in a mechanism for the catalytic action.

Low-temperature rapid synthesis of clathrate hydrates from ice in the presence of some guest substances has been experimentally observed in thin films of ice nanocrystals.^[11] In this respect we note the work of Bobev and Tate, who observed an order of magnitude increase in the rate of methane and CO₂ hydrate formation in the presence of about 10% methanol in the temperature range of 200–250 K.^[12]

Figure 1 shows methane gas uptake (at 253 K and initial methane pressure of 124 bar), as monitored by pressure drop, by the powdered frozen water solutions containing different amounts of methanol, with a total weight of about 3 g. Total monitoring time was 22 h, and it can be seen that the presence of methanol has a remarkable effect on the rate of conversion of ice to hydrate. During this period several of the runs appeared to have reached a steady state (5, 2.5 and 1.2% methanol) in the relatively short time of 4 h. The greatest pressure drop characterizes the largest yield of hydrate, thus it appears that the 1.2% methanol sample showed the greatest degree of conversion. The smaller yields for the 2.5 and 5% methanol samples suggests that most of the methanol is excluded from the hydrate, thus leaving a more concentrated methanol solution to inhibit further hydrate formation. Going up to 10% methanol appears to confirm this, as now the rate of conversion is slower, and the yield is lower than for the other samples. For the 0.6% methanol sample, the overall reaction is slower, but it appears that in the long term the yield will approach that of the 1.2% sample. For this 0.6% sample it appears that there was insufficient methanol to activate all of the ice surface, thus requiring transport of methanol (perhaps in the solid phase) from reacted regions of the sample to those that were not as yet activated.

The pure water sample was very different from the methanol-containing samples in that less than 30% of the sample had converted to hydrate in 22 h if we take the sample with 1.2% methanol as a benchmark. Roughly speaking, this translates into an increase in the rate of the ice–methane reaction for methanol-activated ice prepared from water containing 1.2–5% methanol by two orders of magnitude.

These methane uptake curves can be fit fairly well with exponential decay functions. See the Supporting Information for additional discussions.

According to the methanol–water phase diagram and assuming that there is no methanol trapped in the ice, the frozen samples of methanol solution will consist of ice and a 20% methanol solution at 253 K.^[13] For solutions with original concentrations between 1 and 5% methanol, at 253 K the amount of ice will vary between 95 and 84%, of the sample, respectively. Roughly, this can be taken as the amount of ice that can be converted to hydrate. The remaining water stays in solution to produce a 20% methanol phase. A small amount of methanol can be incorporated in methane hydrate as determined in previous work.^[14,5]

Some of the solid products were characterized by powder X-ray diffraction (PXRD) and Raman spectroscopy. The PXRD pattern in Figure 2a shows that in fact the solid product is almost completely a sI hydrate with very little residual ice remaining in the product. This is in contrast to the hydrate formed from pure ice shown in Figure S4 of the Supporting Information. The lattice constants are slightly smaller than that of the sI methane hydrate made from pure water (Table 1). This may be due to the effect of methanol or ammonia incorporation as hydrogen-bonding clathrate hydrate guests.^[4,5] Our previous work used single-crystal X-ray diffraction and NMR spectroscopy to show the incorpo-

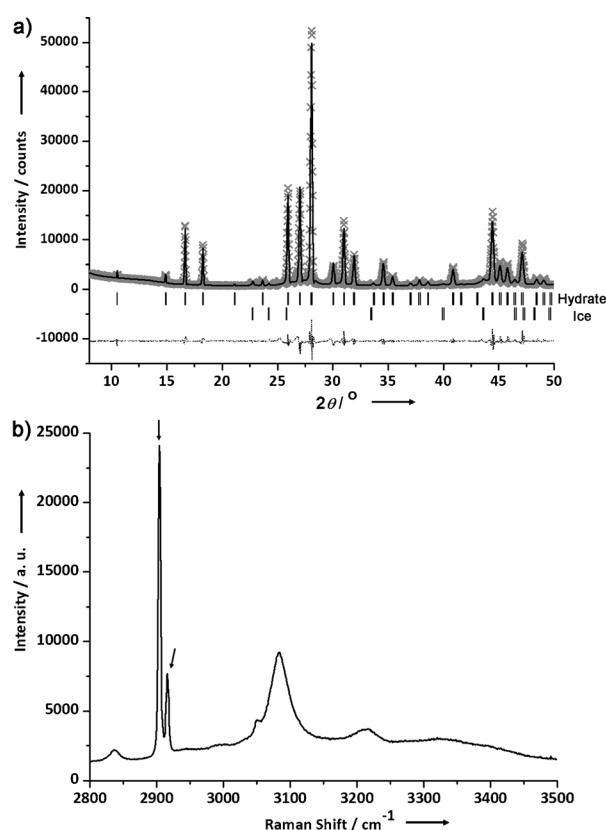


Figure 2. a) Powder X-ray diffraction pattern, b) Raman spectrum in the CH and OH stretch region of the solid hydrate resulting from the reaction of methane with a powdered frozen 5% methanol aqueous solution at –20 °C.

Table 1: Hydrate characterization by PXRD and Raman spectroscopy for pure CH₄ sI hydrate and hydrates formed from ammonia and methanol ice mixtures at -20°C . Lattice parameters are measured at 150 K. The ratio of the area from the peaks for large and small cage guests (A(L)/A(S)) from the Raman spectra were measured at different sites in the sample. Small cage occupancy is also given.

	Pure CH ₄ hydrate, 125 bar	1.4 % NH ₃ solution, 31 bar	2.7 % NH ₃ solution, 125 bar	5 % MeOH solution, 125 bar
lattice parameter [Å]	11.8976(9)	11.8974(6)	11.8804(10)	11.8876(5)
A(L)/A(S), site 1	3.52	3.62	3.24	3.53
A(L)/A(S), site 2	3.61	3.72	2.93	3.53
A(L)/A(S), site 3	3.46	3.62	3.29	3.32
average A(L)/A(S) (small cage occupancy)	3.53 (0.85)	3.65 (0.82)	3.15 (0.95)	3.46 (0.87)

ration of methanol and ammonia in clathrate hydrate phases.^[4,5] The conditions of hydrate synthesis in those articles were similar to those used here.

The Raman spectrum for the C–H and O–H stretch region is shown in Figure 2b. The sharp bands near 2900 cm^{-1} are characteristic of methane in the large and small cages of sI methane hydrate. The integrated band intensities can be used to estimate the methane occupancy ratio and this is close to that obtained for methane hydrate prepared from pure water under the same conditions (see Table 1). The larger fractional occupancy of the methane molecules in the sI small cages (assuming 100% large cage occupancy) in the presence of methanol and ammonia is notable. This does not take into account small quantities of methanol that are included or the effect of encaged methanol on the Raman scattering cross section of methane.

Another set of methane uptake experiments (at 253 K and initial methane pressure of 124 bar) were run with ammonia in aqueous solution rather than methanol. A similar accelerant effect was noted, as seen in Figure 3. The optimum rate of methane hydrate formation was obtained at a concentration of 1.4% ammonia, with the pressure drop completed after about nine hours. Lower concentrations gave slower rates,

although it appears as if about the same long-time yield would be obtained for these slower runs as for the optimum run. A higher concentration (2.7% ammonia) gave the same yield of methane hydrate, but a more complex pressure drop plot than for the optimum run. Some runs were carried out at different methane starting pressures (125, 67, 31 bars) and gave similar accelerated gas uptakes, however, the methane hydrate yields appeared to be better at the lower pressures. Characterization of various samples (Figures S5 and S6 in

the Supporting Information) again showed almost complete conversion to hydrate with little residual ice. The sample with the 2.7% ammonia content gave a smaller lattice parameter, rather similar to the 5% methanol sample, perhaps indicating a stronger guest–host interaction when small quantities of strong hydrogen bonding guests are incorporated. This ammonia sample also showed the largest deviation from the other samples in guest distribution over the hydrate cages. The differences in behavior between the methanol and ammonia solutions could be related to their different uptake in the hydrate phases and the fact that ammonia is seen to substitute water molecules in the hydrate lattice.^[4,5]

Gas uptake runs were also obtained at 253 K with 124 bar methane for frozen aqueous solutions of a variety of other materials that have hydrate inhibitor characteristics, including glycerol, NaOH, NaCl, sucrose, and polyethylene glycol with 2–5 wt% initial concentration, see Figure S1 of the Supporting Information. Although in all cases faster uptake was seen as compared to pure water ice, none showed accelerated uptake comparable to the methanol and ammonia containing solutions. The methane uptake during the pure ice run for this set of experiments shows similar kinetics to the pure ice run used as reference for the methanol and ammonia experiments. This shows the good reproducibility of the method.

The action of methanol and ammonia appears to be unique in accelerating the rate of hydrate formation by up to two orders of magnitude. This leaves us to consider the mechanism by which this “catalytic” action takes place. Of the materials tested, methanol and ammonia have the interesting property of incorporation into some of the hydrate cavities in presence of other guest molecules although they do not form clathrate hydrates themselves in this temperature region because of strong hydrogen bonding interactions with water.^[4,5,15] This makes them effective inhibitors of hydrate formation in aqueous solution at properly adjusted concentration (about 10–50 wt% methanol). However, at lower temperatures, for instance, at -20°C , in the range of methanol concentrations where the catalytic action takes place (about 0.5–5 wt%) ice will form which makes the remaining solutions strongly under-inhibited. The concentration of methanol must approximately be larger than 20% to prevent freezing at this low temperature.

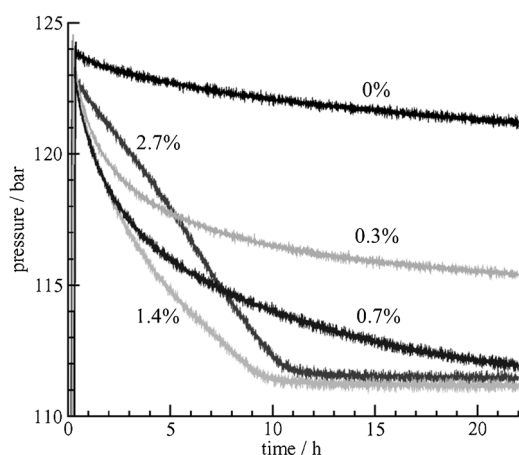


Figure 3. Pressure drop versus time for powdered frozen solutions containing different weight percentages of ammonia in the initial water solution at 253 K.

A full simulation of the experiment would be outside the scope of this initial study. To understand some aspects of the hydrate formation mechanism molecular dynamics simulations were performed on (0001) basal plane of a proton-disordered hexagonal ice Ih phase^[16] coated initially with methanol and exposed to methane gas. Reference simulations were also performed with methane gas in direct contact with the Ih phase. The simulation times are not sufficient to observe the transformation of ice to hydrate, but aspects of this transformation are discerned as described below.

Previous simulation work showed that at temperature below 200 K, methanol forms an ordered monolayer on the (0001) basal plane.^[17] In our simulations, methanol molecules hydrogen bond strongly with the surface water molecules of the Ih surface and lead to the formation of a disordered aqueous methanol phase. Hydrogen bonding between methanol molecules in this aqueous phase with the underlying ice phase helps maintain the hexagonal hydrogen-bonded rings at the ice-solution interface for some time. The *z*-density profile of the simulation after the 20 ns simulation at 210 K and snapshot showing the configuration in the simulation are shown in Figure 4. As the simulation progresses, some water molecules in the first row of the ice lattice can be replaced by methanol molecules that diffuse inwards. Methane gas is concentrated at the methanol solution-ice interface and penetrates a small distance into the water-methanol layer. The *z*-density profiles shown in Figure S2 of the Supporting Information show that methane is also concentrated at a pure ice surface, but the degree of penetration of methane to reach the ice surface is smaller. The progression of the simulation up to 20 ns is shown in Figure S3 of the Supporting Information. Simulations of ammonia on the ice surface also show a region of penetration of the ammonia molecules within the ice lattice.^[11,18] The stronger proton acceptor behavior of ammonia and its different strength of hydrogen bonding and nature of Bjerrum defects caused in the ice lattice show that the details of the diffusion of ammonia into ice may be different from that of methanol.

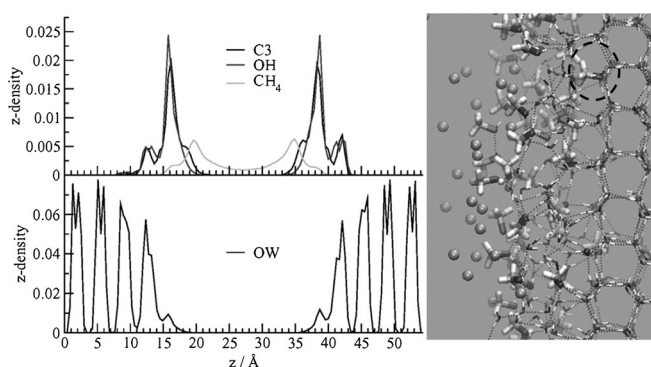


Figure 4. The *z*-density profiles of the methanol carbon (C3), oxygen (OH), methane (CH₄) and water oxygen (OW) from the 20 ns simulation at 210 K. Snapshot of the Ih (0001) basal plane covered with methanol/water and exposed to methane gas. The outer methanol/water is disordered, but methanol in the inner layers can replace a water molecule (see circled molecule) while still maintaining the order in the solid phase.

These observations indirectly suggest a mechanism where methanol molecules, similar to ammonia,^[4] enter the water lattice, but due to the smaller number of hydrogen bonds that methanol forms (three) compared to water (four) there will be Bjerrum defects in the cages which facilitate the entry of methane molecules into the ice lattice. These ice lattice structures may then rearrange to form the canonical cages of the sI methane clathrate hydrate lattice. The other inhibitors listed above cannot be incorporated in the ice phase in the same manner as methanol and ammonia.

Traditional methods of hydrate formation usually involve stirred high pressure reactors where water and gas are contacted under pressure with provision for removing the heat of crystallization (water + gas → hydrate).^[10] The maximum yield is often not more than 10% based on the amount of water used, as stirring the reactor becomes too difficult after solid hydrate formation and an increased viscosity of the water slurry. To isolate the hydrate it has to be separated from the water, followed by pelletization for storage and/or eventual transport. In the process we have explored, the formation of powdered ice/methanol solution can be a completely separate step from the hydrate formation performed at another (unpressurized) part of the facility. When the powdered ice/methanol solution is put in contact with pressurized methane (requiring a lower pressure than in a stirred reactor) hydrate forms quickly. The heat of reaction to hydrate is now only for the (ice + gas → hydrate) reaction, a factor of 6 lower than for the (water + gas → hydrate) reaction using a stirred reactor, and furthermore mechanical stirring is not required. Therefore heat transfer to outside the system during the hydrate formation process is less of a problem than in stirred reactors where hydrate is formed from liquid water. The reactor can be much smaller as the hydrate yield should approach 95%, as opposed to the 10–15% for a stirred reactor. The remaining methanol solution in the hydrate will make the methane hydrate powder compression (to make pellets) much easier than for a dry powder. Of course, the applications for which the hydrate is to be used must tolerate a small quantity of methanol, although most methanol could be flashed off by exposure to a vacuum. Although we have investigated a particular set of conditions (0.6 to 10% methanol concentration and 253 K), the system is tunable in terms of methane pressure, temperature and methanol concentration. Specific values can be adjusted for optimizing hydrate yield, rate of reaction and energy expenditure. In particular, the methanol-water phase diagram can be used to adjust the operating conditions for work at higher temperatures, with corresponding lower energy requirements. Optimization of the reaction conditions may make this method an attractive alternative to the traditional methods of large scale methane hydrate production for storage or transport applications.

The formation of methane hydrate from methanol-ice and ammonia-ice mixtures can have ramifications for flow assurance operations in gas pipelines in cold climates where methanol is added for hydrate inhibition effects. This work shows that inhibition is only operative if ice does not form from the moisture in the system. Any ice that is formed will quickly convert to methane hydrate in the presence of the

methanol solution present in the pipeline. This work also provides an additional mechanism for methane hydrate formation in the cold and relatively low methane pressure environments of planetary bodies, in particular Saturn's moons Titan and Enceladus. The known presence of ice and aqueous ammonia/methanol solutions can catalyze the formation of methane hydrate, even in the low methane pressure atmospheres of these moons. The prevalence of methane hydrates could provide an explanation for the persistence of methane gas in these moons, despite the fact that escape velocities would suggest methane should have long escaped their atmospheres.^[19]

Received: March 24, 2014

Published online: August 11, 2014

Keywords: gas uptake · hydrates · methanol · molecular dynamics · powder x-ray diffraction

- [1] S. Alavi, K. Udachin, C. I. Ratcliffe, J. A. Ripmeester, *Clathrate Hydrates in Supramolecular Chemistry from Molecules to Nanomaterials* (Eds.: P. A. Gale, J. W. Steed), Wiley, Hoboken, **2012**.
- [2] A. V. Milkov, *Earth-Sci. Rev.* **2004**, *66*, 183–197.
- [3] E. D. Sloan, C. A. Koh, *Clathrate Hydrates of Natural Gases*, 3rd ed. CRC, Boca Raton, FL, **2007**.
- [4] K. Shin, R. Kumar, K. A. Udachin, S. Alavi, J. A. Ripmeester, *Proc. Natl. Acad. Sci. USA* **2012**, *109*, 14785–14790.
- [5] K. Shin, K. A. Udachin, I. L. Moudrakovski, D. M. Leek, S. Alavi, C. I. Ratcliffe, J. A. Ripmeester, *Proc. Natl. Acad. Sci. USA* **2013**, *110*, 8437.
- [6] J. H. van der Waals, J. C. Platteeuw, *Adv. Chem. Phys.* **1959**, *2*, 1–57.
- [7] a) R. Ohmura, S. Takeya, T. Uchida, T. Ebinuma, *Ind. Eng. Chem. Res.* **2004**, *43*, 4964; b) T. Maekawa, *Fluid Phase Equilib.* **2008**, *267*, 1; c) A. Chapoy, R. Anderson, H. Haghighi, T. Edwards, B. Tohidi, *Ind. Eng. Chem. Res.* **2008**, *47*, 1689; d) K. Yasuda, S. Takeya, M. Sakashita, H. Yamawaki, R. Ohmura, *Ind. Eng. Chem. Res.* **2009**, *48*, 9335; e) K. A. Udachin, S. Alavi, J. A. Ripmeester, *J. Chem. Phys.* **2011**, *134*, 121104; f) P. S. R. Prasad, T. Sugahara, A. K. Sum, E. D. Sloan, Jr., C. A. Koh, *J. Phys. Chem. A* **2009**, *113*, 6540; g) D. Y. Kim, J. Lee, Yu.-T. Seo, J. A. Ripmeester, H. Lee, *Angew. Chem.* **2005**, *117*, 7927–7930; *Angew. Chem. Int. Ed.* **2005**, *44*, 7749–7752; h) D. Y. Kim, Y. Park, H. Lee, *Catal. Today* **2007**, *120*, 257–261.
- [8] E. G. Hammerschmidt, *Oil Gas J.* **1939**, *37*, 66–71.
- [9] P. D. Menten, W. R. Parrish, E. D. Sloan, *Ind. Eng. Chem. Process Des. Dev.* **1981**, *20*, 410–413.
- [10] a) P. Englezos, *Rev. IFP* **1996**, *51*, 789; b) Y.-T. Seo, I. L. Moudrakovski, J. A. Ripmeester, J.-W. Lee, H. Lee, *Environ. Sci. Technol.* **2005**, *39*, 2315–2319; c) L. C. Ho, P. Babu, R. Kumar, P. Linga, *Energy* **2013**, *63*, 252–259; d) P. Babu, R. Kumar, P. Linga, *Int. J. Greenhouse Gas Control* **2013**, *17*, 206–214.
- [11] a) K. D. Williams, J. P. Devlin, *J. Mol. Struct.* **1997**, *104*, 5770–5777; b) N. Uras, J. P. Devlin, *J. Phys. Chem. A* **2000**, *104*, 5770–5777; c) D. B. Gulluru, J. P. Devlin, *J. Phys. Chem. A* **2006**, *110*, 1901–1906.
- [12] S. Bobev, K. T. Tait, *Amer. Miner.* **2004**, *89*, 1208–1214.
- [13] G. A. Miller, D. K. Carpenter, *J. Chem. Eng. Data* **1964**, *9*, 371–373.
- [14] A. Wallqvist, *J. Chem. Phys.* **1992**, *96*, 5377–5382.
- [15] a) F. E. Anderson, J. M. Prausnitz, *AIChE J.* **1986**, *32*, 1321–1333; b) Y. Yamamoto, K. Nagashima, T. Kornai, A. Wakisaka, *Ann. N. Y. Acad. Sci.* **2000**, *912*, 797–806.
- [16] J. A. Hayward, J. R. Reimers, *J. Chem. Phys.* **1997**, *106*, 1518–1529.
- [17] a) S. Picaud, C. Toubin, C. Girardet, *Surf. Sci.* **2000**, *454*–456, 178–182; b) P. Jedlovsky, L. Pártay, P. N. M. Hoang, S. Picaud, P. von Hessberg, J. N. Crowley, *J. Am. Chem. Soc.* **2006**, *128*, 15300–15309; c) B. Collignon, S. Picaud, *Chem. Phys. Lett.* **2004**, *393*, 457–463.
- [18] a) J. P. Devlin, V. Buch, *J. Phys. Chem. A* **1997**, *101*, 6095–6098; b) H. Ogasawara, N. Horimoto, M. Kawai, *J. Chem. Phys.* **2000**, *112*, 8229–8232.
- [19] a) M. Choukroun, O. Grasset, G. Tobie, C. Sotin, *Icarus* **2010**, *205*, 581–593; b) C. C. Porco, et al., *Science* **2006**, *311*, 1393–1401; c) A. D. Fortes, E. R. Stofan, *36th Lunar and Planetary Science Conference* **2005**, abstr 1123.